

Modeling Rebar in Reinforced Concrete for ALE Simulations

Shih Kwang TAY, Jiing Koon POON and Roger CHAN

Ministry of Home Affairs, Singapore

Abstract

*A constraint based method to couple rebar in reinforced concrete has been a popular method for Lagrangian simulations. However modeling rebar in Arbitrary Lagrangian-Euler (ALE) concrete has not been widely documented. This paper aims to investigate the effectiveness of the two constraint based keywords, *ALE_COUPLING_NODAL_CONSTRAINT and *CONSTRAINED_LAGRANGE_IN_SOLID found in LS-DYNA[®] to couple beam elements in ALE concrete. This paper also explores the option of explicitly assigning steel rebar material within the ALE concrete using *INITIAL_VOLUME_FRACTION to create a Multi-Material Arbitrary Lagrangian-Euler (MM-ALE) simulation.*

Introduction

Reinforced concrete (RC) is commonly used in the construction of protective structures. To accurately simulate the response of RC structures in numerical models, it is crucial that the steel reinforcements embedded in the concrete are correctly represented in the models. In Lagrangian RC models, the *CONSTRAINED_LAGRANGE_IN_SOLID (CLIS) keyword is commonly used to couple reinforcement (modeled using beam elements) nodes to the concrete nodes. This is often the preferred method as compared to the shared-node approach, as it does not require the nodes for the concrete elements and the reinforcement elements to coincide in space i.e. they can be meshed independently.

Though modeling rebar in Arbitrary Lagrangian-Euler (ALE) concrete using similar constraint-based method has not been widely documented, it is not entirely unheard of and was performed in an ALE RC column against explosive loading [1]. On a separate note, the LS-DYNA manual [2] cited that *ALE_COUPLING_NODAL_CONSTRAINT (ACNC) keyword can also apply constraint conditions for steel reinforcement in concrete and went further to encourage users to use this keyword instead of CLIS. It is therefore of interest to study the various approaches in modeling rebar in concrete for ALE element formulation.

This paper shares the findings gathered from a series of uniaxial extension of ALE RC slab that was previously studied using the Lagrangian approach reported in [3] and presents a case-study comparing simulation results from various coupling methods with a 3-point bending test. Taking cognizance that ALE approach was developed with the intent to simulate short duration problems with high pressure and velocity gradients and essentially not suited for such long duration problem, we understood that quasi-static problems might not be the best way to verify this approach. Nevertheless, quasi-static problems are less complex than dynamic problems, and understanding the use of ALE approach for such problems is beneficial before we move on to more complex dynamic problems, especially those involving close-in blast loads.

*Mat72R3 (Karagozian & Case (K&C) Concrete Model Release 3) was used as the concrete material model in continuation of earlier work reported in [4].

Motivation

As part of Ministry of Home Affairs (MHA) Singapore long-term technology development programme to study close-in, contact and near contact blast effects on structural elements as well as the mechanism of progressive collapse [5, 6, 7], MHA had shared some of the simulation work to study blast effects on structural elements via the Lagrangian approach and subsequently via the ALE approach [4]. To further investigate ALE techniques as a viable alternative to Lagrangian approach, the work presented in this paper aims to investigate rebar coupling in Eulerian concrete as part of the component testing prior to going into a full-scale ALE reinforced concrete column model.

Slab Axial Extension Investigation

An axial extension of an ALE RC slab was conducted similar to the model setup described in [3]. Schwer (2013) noted that for the Lagrangian slab model, both the CLIS and ACNC constraint methods do not provide additional axial force beyond that of the concrete failing in tension. The intent of this series of simulation was to investigate if this finding was similarly observed in an ALE model.

Three key models were created:

Model I: Lagrangian concrete (Mat84/85) solid elements with steel beam elements (Mat24) coupled using CLIS – essentially the same as the model in [3] so as to check our model accuracy

Model II: ALE concrete (Mat72R3) with steel beam elements (Mat24) coupled using CLIS/ACNC – this is to check whether the beam elements can be coupled with ALE concrete and whether the findings reported in [3] applies to an ALE model

Model III: ALE concrete (Mat72R3) with rebar (Mat24) elements modeled using *INITIAL_VOLUME_FRACTION_GEOMETRY – this is to check if the rebar can contribute to the axial tension capacity if modeled as ALE (Figure 1)

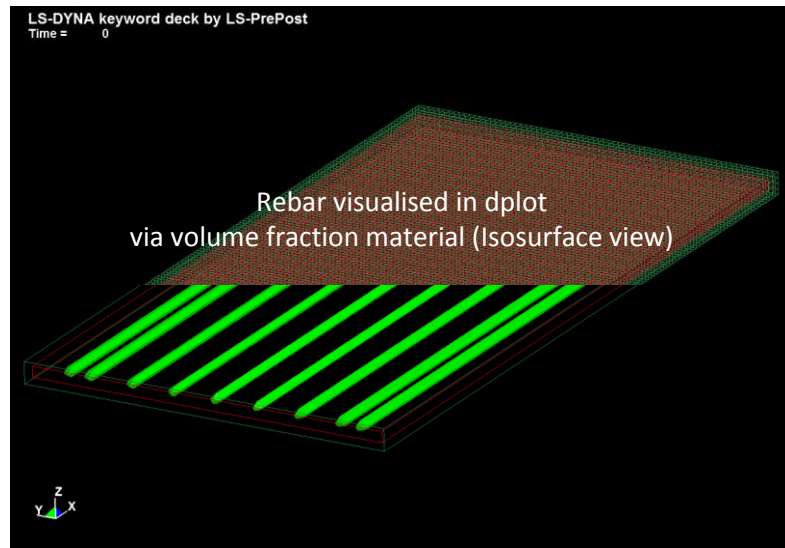


Figure 1: Model III: MMALE Concrete and Rebars

The boundary conditions for the models followed the same boundary conditions prescribed by [3]. As explained in details in [3], a group of concrete only nodes interior to the edges of the slab were selected as shown in Figure 2. The X-forces at all the SPC nodes were output via *DATABASE_SPCFORC and summed to provide the total X-force. Figure 3 compares the results from the various axial extension runs.

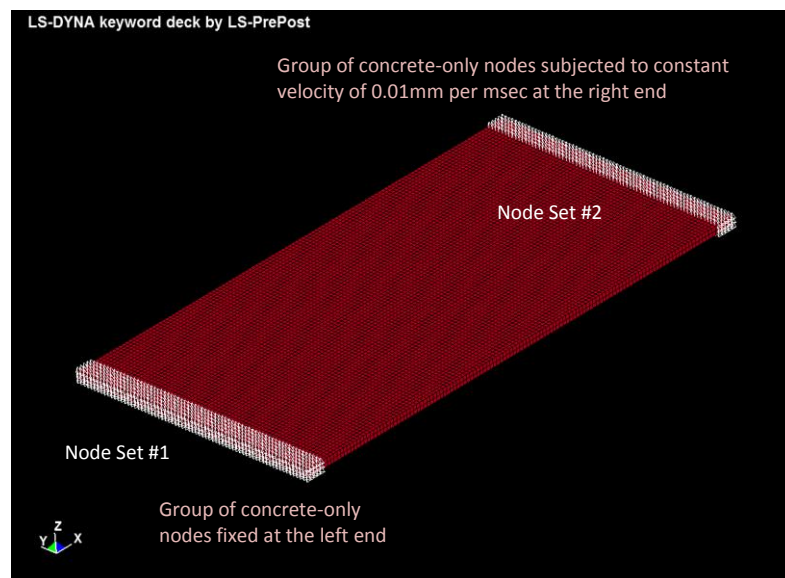


Figure 2: Boundary Conditions

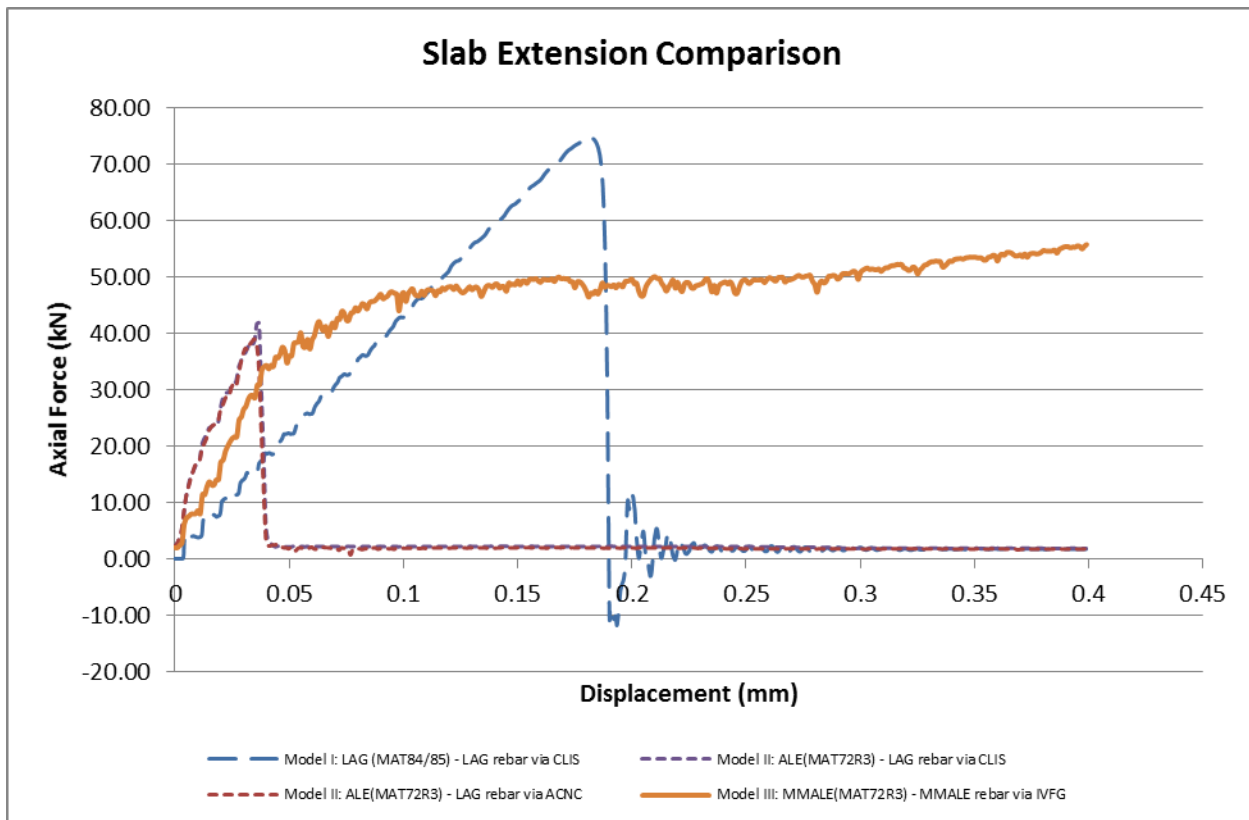


Figure 3: Comparison of Results

As mentioned earlier, Model I was created to compare with the results reported in [3]. The peak axial force for Model I was 74.7kN@0.18mm, slightly below 82.3kN@0.2mm reported in [3]. The main takeaway was that it was similarly observed in Model I that the rebar do not contribute to axial capacity once the concrete failed in tension.

The recorded axial force in Model II peaked at 41.7kN@0.036mm, much lower and at a lower displacement than the reported Lagrangian model. This finding is not well understood and needs further investigation on the tensile behavior of ALE concrete. Similar to the Lagrangian model, it was also observed in the ALE model that the Lagrangian rebar coupled using CLIS and ACNC do not contribute to axial capacity once concrete failed in tension as well.

However, in Model III, it can be seen in Figure 3 that the rebar, when modeled as ALE elements, indeed contributed to the resistance beyond the concrete tensile capacity, although the recorded axial force is still lower than that reported for shared-node beams in [3].

A mesh refinement was conducted to see if the results improve with a mesh size half of the original. Figure 4 showed that the refined model achieved an even lower strength compared to the base model, although the behavior seemed similar. An earlier study [4] on ALE concrete compressive strength reported that the strength moved closer to the input values when the mesh was refined. It was therefore surprising to find that the results of mesh refinement in this study turned out to be counter-intuitive.

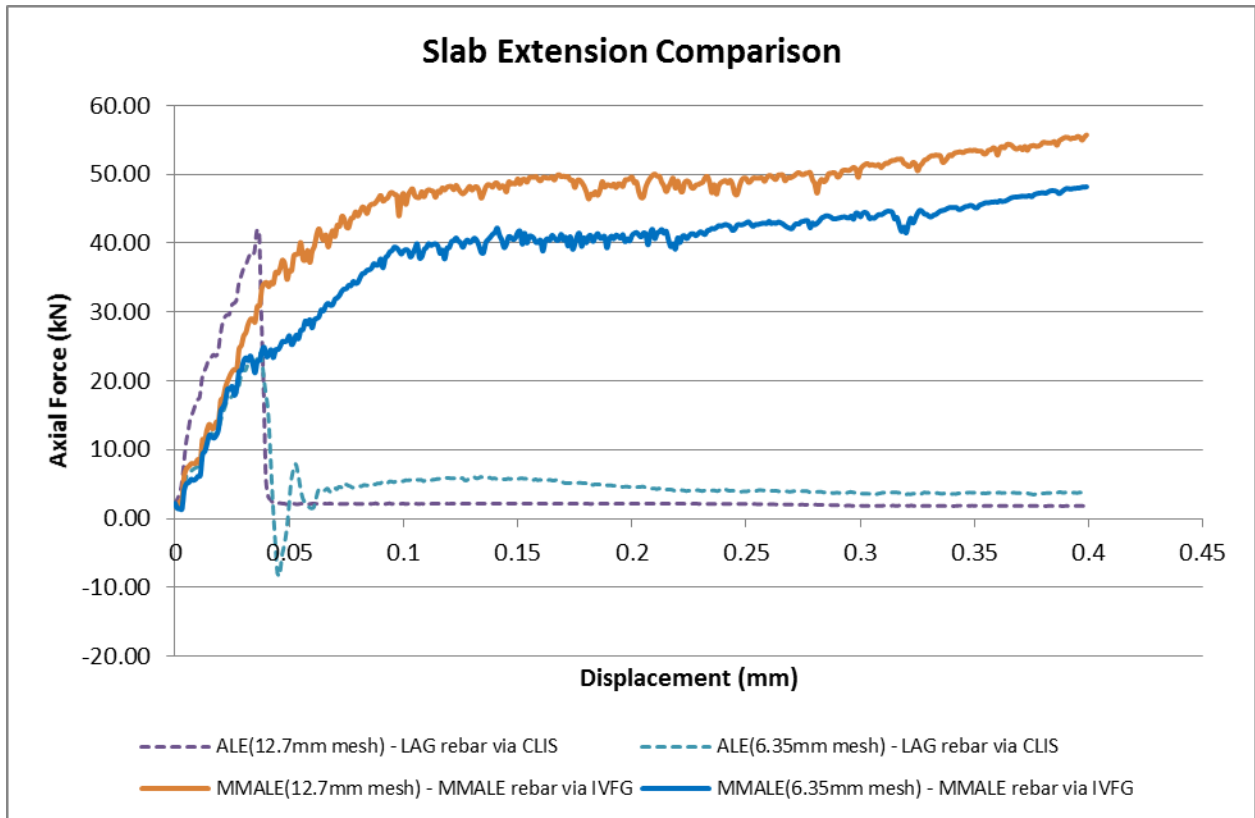


Figure 4: Comparison of Results – Mesh Size

Three Point Bending Test – Case Study

After observing that beam elements coupled with ALE concrete using constraint-based methods such as CLIS and ACNC similarly seemed to ignore the contribution of the reinforcement to the tensile capacity of RC components, a further study was conducted to compare the various methods of modeling rebar in an ALE model. A three-point bending test was selected as a case study as there was experimental data to compare against the simulation results. Lagrangian RC models were similarly set up for the purpose of comparing both modeling approaches.

The intent of this exercise was not to comprehensively describe all the complex interactions between the reinforcement and concrete, but rather it was to gain more insights on the various coupling methods available in LS-DYNA so that such findings could be used in future to guide the model set up for the full-scale ALE RC column.

Model Geometry

The RC beam model was set up as described in [8] and as shown in Figure 5. A concrete beam with no rebar was created as a base model and two reinforcement ratios were selected for the case study, namely 0.25% that consisted of one $\phi 8$ rebar and 0.50% that consisted of two $\phi 8$ rebar. A consistent mesh size of 10mm was adopted for all solid and beam elements. This allowed the rebar nodes to coincide with the concrete model and facilitated the geometry creation for the shared-node approach.

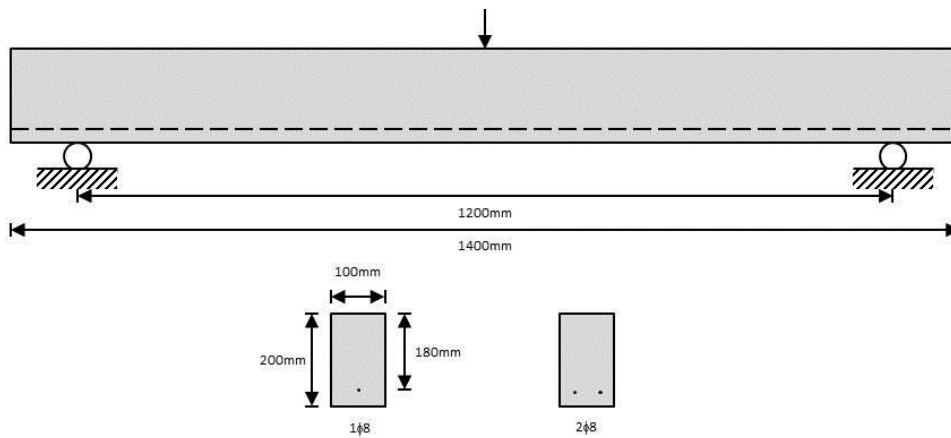


Figure 5: Geometry of specimens

The concrete beam and air domains were separately created for the ALE model and defined using ELFORM=11 (1-point ALE multi-material element). Mat72R3 was selected as the concrete material model and its parameters were generated based on a cylinder strength $f_c' = 36.75\text{MPa}$. The Grade 60 reinforcement bars were defined using ELFORM=1 (Hughes-Liu) beam elements and Mat24 (Piecewise Linear Plasticity) was used as the constitutive model with *DEFINE_TABLE to specify the effective plastic strain values vs effective stress values at various strain rates.

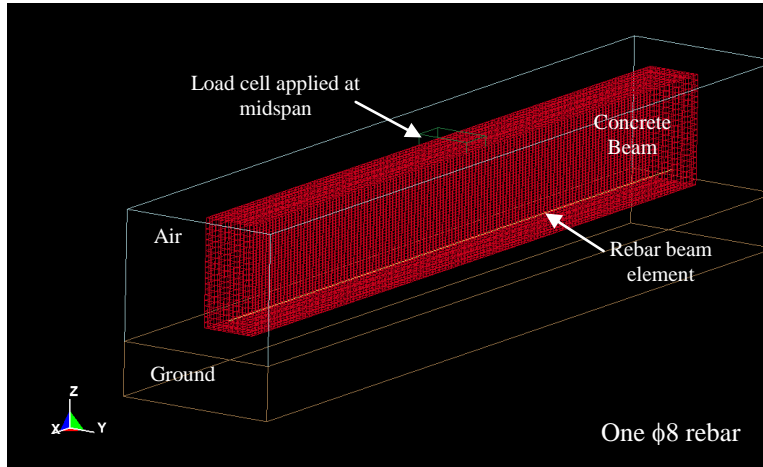


Figure 6a: Model of the ALE RC beam for coupling methods using CLIS, ACNC and shared-node approach

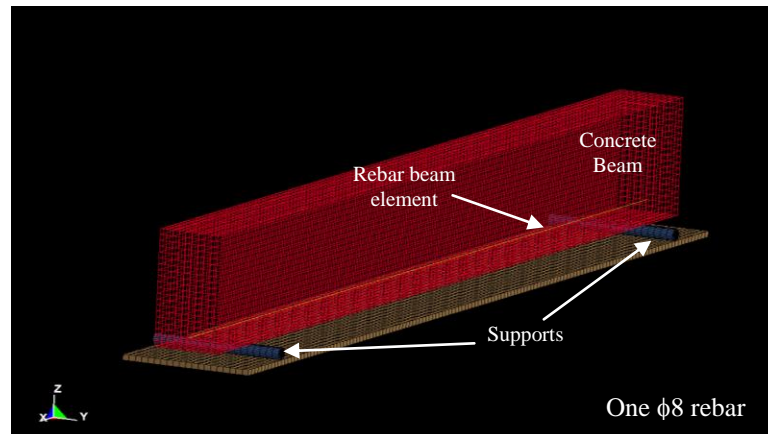


Figure 6b: Model of the Lagrangian RC beam for coupling methods using CLIS, ACNC and shared-node approach

Boundary Conditions

Defining the support condition for the Lagrangian model was more straightforward as compared to the ALE model. The supports for the Lagrangian model were explicitly modeled as cylinders and constrained in space. *CONTACT_AUTOMATIC_SURFACE_TO_SURFACE keyword was inserted to define the contact between the RC beam and the supports. The supports for the ALE model, on the other hand, was partitioned out of the air domain using *INITIAL_VOLUME_FRACTION_GEOMETRY (IVFG). As both the supports and RC beam were modeled in ALE, they interacted automatically and it was not necessary to define or impose any controls.

For the load application, *LOAD_SEGMENT_SET was directly applied to the mid-span of the Lagrangian RC beam as seen in Figure 7b. As for the ALE model, a loading block made up of ALE solid elements was created above the midspan of the RC beam where the segment load was applied on. This was done to accommodate the IVFG approach which will be discussed later in the paper. The load was applied at a rate of 100N/ms in the simulation runs as opposed to the deflection rate of $8\mu\text{ms}^{-1}$ cited in the bending test in order to achieve an optimal computational cost that existing in-house computational capability could offer. Loading rate sensitivity was separately investigated and shared in the later part of the paper.

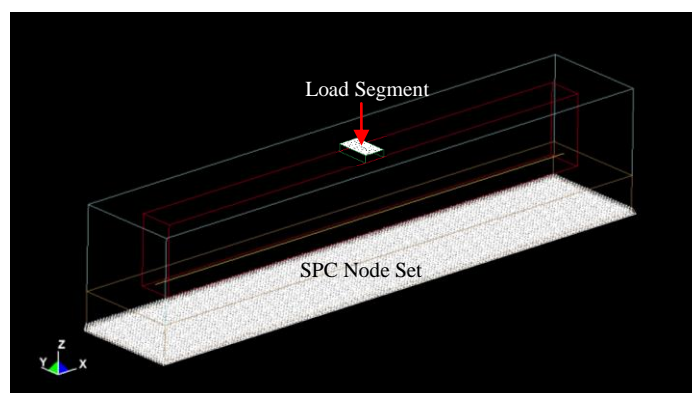


Figure 7a: Boundary Conditions for ALE Model

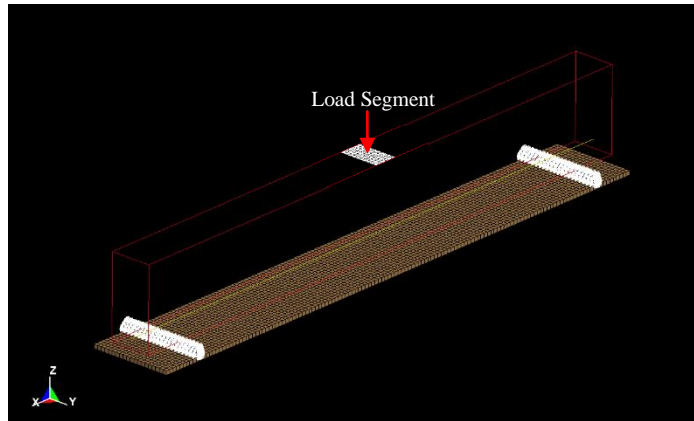


Figure 7b: Boundary Conditions for Lagrangian Model

Rebar Modeling Approaches

The following models were created with various methods to include the reinforcement. For the constraint-based methods, similar CLIS and ACNC parameters were used for both the ALE and Lagrangian models.

ALE Model	Lagrangian Model
Model A0: No Rebar	Model B0: No Rebar
Model A1-1: 1φ8 CLIS coupling	Model B1-1: 1φ8 CLIS coupling
Model A1-2: 1φ8 ACNC coupling	Model B1-2: 1φ8 ACNC coupling
Model A1-3: 1φ8 Shared-Nodes	Model B1-3: 1φ8 Shared-Nodes
Model A1-4: 1φ8 IVFG	
Model A2-1: 2φ8 CLIS coupling	Model B2-1: 2φ8 CLIS coupling
Model A2-2: 2φ8 ACNC coupling	Model B2-2: 2φ8 ACNC coupling
Model A2-3: 2φ8 Shared-Nodes	Model B2-3: 2φ8 Shared-Nodes
Model A2-4: 2φ8 IVFG	

The shared-node approach does not require any additional keywords except to merge the coincident nodes between the reinforcement and concrete mesh in LS-PrePost[®]. However it should be noted that the shared nodes method will lead to non-physical results in the ALE models, as the reinforcement will be fixed in space within the concrete mesh and may not be able to respond well as the concrete material advect. As seen in Figure 8, the results of the merged nodes method came as no surprise, where there was distortion in the mesh when the rebar beam elements deflected and it was doubtful if the results could be trusted.

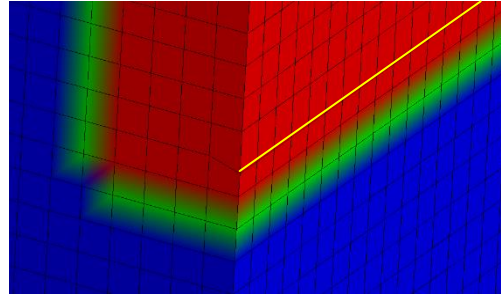


Figure 8: Distortion in the mesh for the shared nodes method when the ALE RC beam deflects

Explicit modeling of solid element rebar in a Lagrangian concrete model requires extensive modeling and computational efforts. However modeling the steel rebars in ALE concrete can be easily achieved with IVFG keyword where user can use various geometry types to define the volume fractions with various ALE multi-material groups (AMMG). As the concrete beam created by the IVFG keyword could not be visualized in LS-PrePost before initialization, it was not possible to define the segment set on which the load would be applied in LS-PREPOST. To overcome this limitation, a block of ALE solid elements (where the load would be applied) was created just above and in contact with the midspan of the RC beam for the load application on the beam.

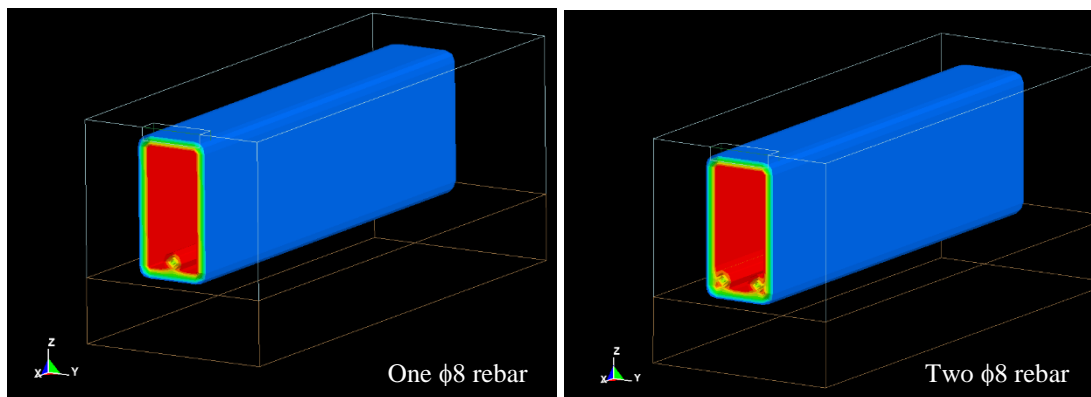


Figure 9: Model of the MM-ALE RC beam using IVFG (Rebar visualised in dplot via volume fraction material (Isosurface view))

Results

Figures 10 and 11 show the load-deflection curves for the one rebar and two rebar models respectively. As expected, both Lagrangian and ALE models behaved in a linear, elastic manner up to the cracking load. The Lagrangian models exhibited a cracking load closer to the experimental data as opposed to the ALE models, which under-predicted the strength of the RC beam in various stages of the load-deflection curve. It was also observed that the load-deflection curves for the Lagrangian models behave similar to one another regardless of the method of rebar modeling. As a general trend, it was noted that hourglass energy increases exponentially in the Lagrangian models beyond the cracking load, where the ratio of the Hourglass energy to Internal energy instantaneously exceeds 10%, making the results beyond this point doubtful [9]. Since the study was focused on the ALE models, there were no further attempts to reduce hourglassing.

The ALE Models A1-2 and A2-2 (with rebars coupled using ACNC) appeared to be stiffer, resulting in a lower cracking load than the models with rebars coupled using CLIS. It can be seen from the chart that Models A1-4 and A2-4 (with rebars modeled as ALE using IVFG) displayed significantly higher strength as compared to other ALE models. This could likely be due to more significant contribution of the rebars (beyond concrete failure) when they were modeled using IVFG, as seen in the slab extension case discussed earlier. This model also responded in an “elastoplastic” manner after first yield as opposed to other models that developed a plastic response.

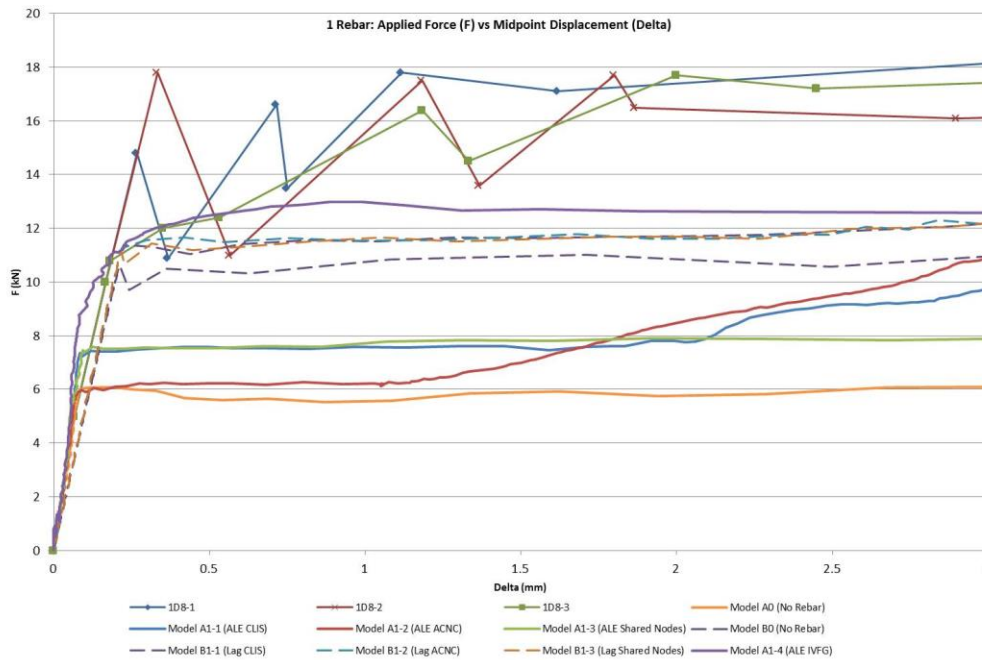


Figure 10: Load-Deflection Curves for One Rebar RC Beam

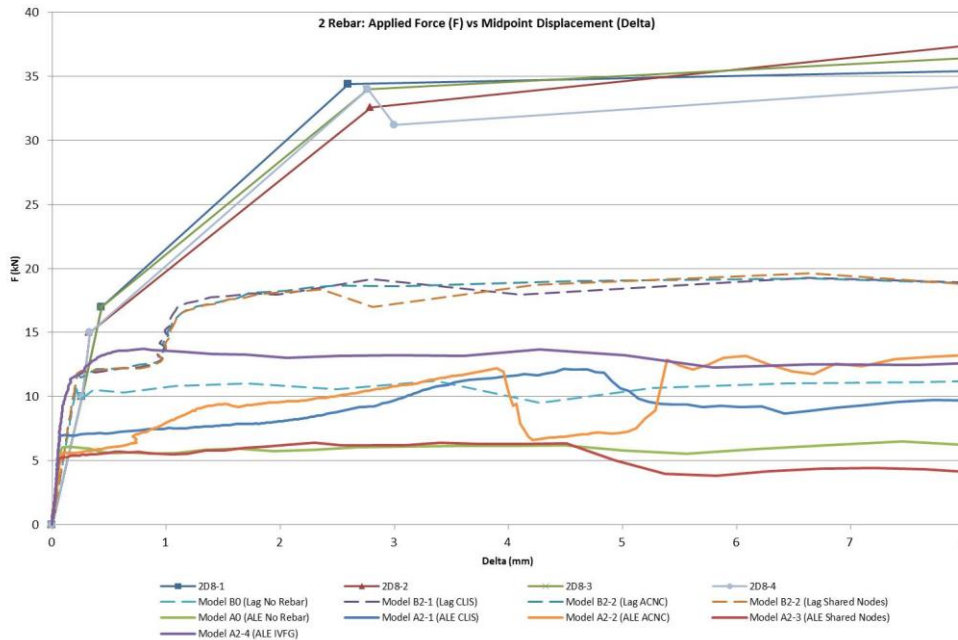


Figure 11: Load-Deflection Curves for Two Rebar RC Beam

Loading rate sensitivity was briefly investigated on the one-rebar models coupled using CLIS. Referring to Figure 12, the Lagrangian models achieved relatively close cracking load with varying loading rate and were also comparable to experiment data. However it can be seen that the ALE models were very sensitive to loading rate and showed no signs of convergence.

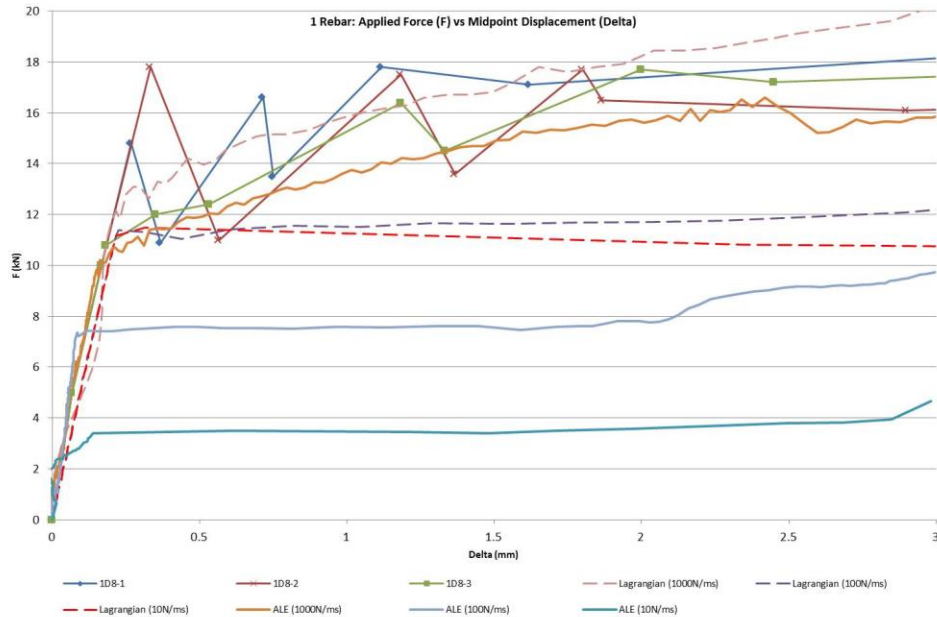


Figure 12: Loading rate comparison for one rebar Lagrangian and ALE models modeled using CLIS

Mesh Refinement

A mesh refinement procedure as described in [10] was conducted on the one rebar Lagrangian and ALE model coupled using CLIS. GCI calculations for solution verification for cracking load were presented. GCI of <10% were obtained and this implied that convergence had been reasonably achieved.

Lagrangian Model

GCI Check	Load ₁₅	Load ₁₀	Load ₅	Load _{Extrapolated}	P	GCI _{5/10}	95% Confidence Interval
Cracking Load (kN)	12.383	11.376	10.795	10.615	2.079	2.09%	[10.570, 11.020]

ALE Model

GCI Check	Load ₂₀	Load ₁₀	Load ₅	Load _{Extrapolated}	P	GCI _{5/10}	95% Confidence Interval
Cracking Load (kN)	11.451	7.207	6.553	6.530	4.893	0.43%	[6.525, 6.581]

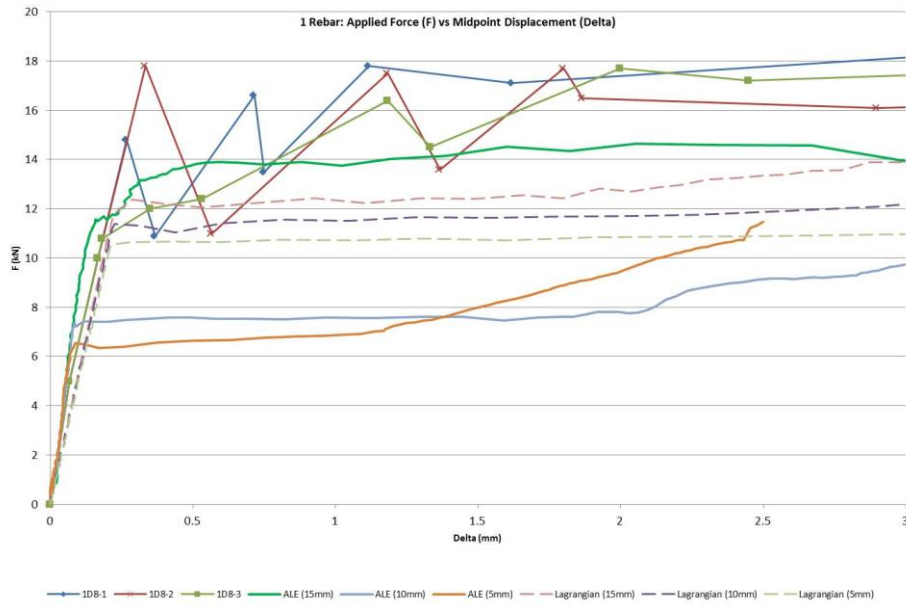


Figure 13: Mesh refinement for one rebar Lagrangian and ALE models modeled using CLIS

Conclusion

The ALE slab extension example observed that CLIS and ACNC constraint methods do not provide additional axial force beyond that of the concrete failing in tension, similar to that reported for a Lagrangian model. It was also demonstrated that ALE rebar modeled using IVFG contributed to the resistance beyond the concrete tensile capacity. It was thus not surprising to see the RC beam with ALE rebar displaying higher loading capacity in the three-point bending case study as compared to other rebar coupling methods.

While the simulation results were unable to match experimental data due to the inherent application of ALE solver to model short-duration problem, it suggested that validation cases with extreme loading regime i.e. blast loading, would provide a better basis for comparison.

References

- [1] John M. H. Puryear, David J. Stevens, Kirk A. Marchand, Eric B. Williamson, C. Kennan Crane. "ALE Modeling of Explosive Detonation on or near Reinforced-Concrete Columns", 12th International LS-DYNA Users Conference, 2012
- [2] LS-DYNA 971 R6.1.0 Keyword Manuals I & II, 2012
- [3] Len Schwer. "Modeling Rebar: The Forgotten Sister in Reinforced Concrete Modeling", 13th International LS-DYNA Users Conference, 2013
- [4] Swee Hong Tan, Roger Chan, Jiing Koon Poon, David Chng. "Verification of Concrete Material Models for MM-ALE Simulations", 13th International LS-DYNA Users Conference, 2013
- [5] Swee Hong Tan, Jiing Koon Poon, Roger Chan, David Chng. "Retrofitting of Reinforced Concrete Beam-Column via Steel Jackets against Close-in Detonation", 12th International LS-DYNA Users Conference, 2012
- [6] Swee Hong Tan, Shih Kwang Tay, Jiing Koon Poon, David Chng. "Fluid-Structure Interaction involving Close-in Detonation Effects on Column using LBE MM-ALE Method", 9th European LS-DYNA Users Conference, 2013

- [7] Jiing Koon Poon, Roger Chan, David Chng. “Contact and Near-Contact Detonation on Concrete Components”, 15th International Symposium on Interactions of the Effects of Munitions on Structures (ISIEMS), 2013
- [8] Alberto Carpinteri, Jacinto Ruiz Carmona, Giulio Ventura. “Failure Mode Transitions in Reinforced Concrete Beams – Part 2: Experimental Tests”, ACI Structural Journal, May-June 2011
- [9] www.dynasupport.com
- [10] “Standard for Verification and Validation in Computational Fluid Dynamics and Heat Transfer”, ASME, 2009.

Input parameters for the ALE Model presented in case study

```
*MAT_CONCRETE_DAMAGE_REL3
$# mid ro pr
$ 1 0.002120 0.200000
$ f't A0 A1 A2 B1 OMEGA A1F
3.324E+00 1.086E+01 4.463E-01 2.199E-03 1.600E+00 5.000E-01 4.417E-01
$ sLambda NOUT EDROP RSIZE UCF LCRate LocWidth NPTS
1.000E+02 2.000E+00 1.000E+00 3.973E-02 1.450E+02 0.000E+00 6.000E+01 1.300E+01
$ Lambda01 Lambda02 Lambda03 Lambda04 Lambda05 Lambda06 Lambda07 Lambda08
0.000E+00 8.000E-06 2.400E-05 4.000E-05 5.600E-05 7.200E-05 8.800E-05 3.200E-04
$ Lambda09 Lambda10 Lambda11 Lambda12 Lambda13 B3 AOY A1Y
5.200E-04 5.700E-04 1.000E+00 1.000E+01 1.000E+10 1.150E+00 8.203E+00 6.250E-01
$ Eta01 Eta02 Eta03 Eta04 Eta05 Eta06 Eta07 Eta08
0.000E+00 8.500E-01 9.700E-01 9.900E-01 1.000E+00 9.900E-01 9.700E-01 5.000E-01
$ Eta09 Eta10 Eta11 Eta12 Eta13 B2 A2F A2Y
1.000E-01 0.000E+00 0.000E+00 0.000E+00 0.000E+00 1.350E+00 3.219E-03 7.007E-03
*EOS_TABULATED_COMPACTIION
$ EOSID Gamma E0 Vol0
$# eosid gama e0 vo
$ 8 0.000 0.000 1.000000
$ VolStrain01 VolStrain02 VolStrain03 VolStrain04 VolStrain05
0.000000000E+00 -1.500000000E-03 -4.300000000E-03 -1.010000000E-02 -3.050000000E-02
$ VolStrain06 VolStrain07 VolStrain08 VolStrain09 VolStrain10
-5.130000000E-02 -7.260000000E-02 -9.430000000E-02 -1.740000000E-01 -2.080000000E-01
$ Pressure01 Pressure02 Pressure03 Pressure04 Pressure05
0.000000000E+00 2.39132322E+01 5.21308461E+01 8.36963126E+01 1.59022994E+02
$ Pressure06 Pressure07 Pressure08 Pressure09 Pressure10
2.39849719E+02 3.40285294E+02 5.20591064E+02 3.03937181E+03 4.64873233E+03
$ Multipliers of Gamma*E
.000000000E+00 .000000000E+00 .000000000E+00
.000000000E+00 .000000000E+00 .000000000E+00
$ BulkUnld01 BulkUnld02 BulkUnld03 BulkUnld04 BulkUnld05
1.59421548E+04 1.59421548E+04 1.61653449E+04 1.69783948E+04 2.01987101E+04
$ BulkUnld06 BulkUnld07 BulkUnld08 BulkUnld09 BulkUnld10
2.34349675E+04 2.66552828E+04 2.90944325E+04 6.54584875E+04 7.97107739E+04
*MAT_PIECEWISE_LINEAR_PLASTICITY
$# mid ro e pr sigy etan fail tdel
$ 9 0.007860 2.0000E+5 0.300000 475.85999 0.000 0.000 0.000
$ c p lcss lcsr vp
0.000 0.000 6000 0 1.000000
$ eps1 eps2 eps3 eps4 eps5 eps6 eps7 eps8
0.000 0.000 0.000 0.000 0.000 0.000 0.000 0.000
$ es1 es2 es3 es4 es5 es6 es7 es8
0.000 0.000 0.000 0.000 0.000 0.000 0.000 0.000
```

CLIS

```
*CONSTRAINED_LAGRANGE_IN_SOLID
$# slave master sstyp mstyp nquad ctype direc mcoup
$ 9 1 1 1 0 2 2 0
$ start end pfac fric frcmin norm normtyp damp
0.0001.0000E+10 0.100000 0.000 0.500000 0 0 0.000
$ cq hmin hmax ileak pleak lcldpor nvent blockage
0.000 0.000 0.000 0 0.100000 0 0 0
$ iboxid ipenchk intforc iale sof lagmul pfacmm thkf
0 0 0 0 0.000 0 0.000
```

ACNC

```
*ALE_COUPLING_NODAL_CONSTRAINT_ID
$# coupid title
$ 1
$ slave master stype mtype ctype mcoup
$ 9 1 1 1 2 0
$ start end frcmin
0.0001.0000E+10 0 0 0 0.500000
```

IVFG

```
*INITIAL_VOLUME_FRACTION_GEOMETRY
$# fmsid fmidtyp bamng ntrace
$ 99 1 3 3
$# conttyp fillopt famng vx xy xz radvel unused
$ 5 0 1 0.000 0.000 0.000 0 0
$# xmin ymin zmin xmax ymax zmax unused unused
-700.00000-50.000000 0.000 700.00000 50.000000 200.00000
$# conttyp fillopt famng vx xy xz radvel unused
$ 4 0 4 0.000 0.000 0.000 0 0
$# x1 y1 z1 x2 y2 z2 r1 r2
-600.00000-100.00000-10.000000-600.00000 100.00000-10.000000 10.000000 10.000000
$# conttyp fillopt famng vx xy xz radvel unused
$ 4 0 4 0.000 0.000 0.000 0 0
$# x1 y1 z1 x2 y2 z2 r1 r2
600.00000-100.00000-10.000000 600.00000 100.00000-10.000000 10.000000 10.000000
$# conttyp fillopt famng vx xy xz radvel unused
$ 4 0 5 0.000 0.000 0.000 0 0
$# x1 y1 z1 x2 y2 z2 r1 r2
-700.00000 0.00000 20.000000 700.00000 0.00000 20.000000 8.000000 8.000000
```

Fill ALE air mesh with AMMG 1 (concrete) using CONTTYP = 5 (Rectangular Box)

Creating supports at two ends of the concrete

Fill the concrete with AMMG 5 (steel rebar) using CONTTYP = 4 (Cylinder)